Response behavior of diblock copolymer brushes in explicit solvent

Kai Gong, Bennett D. Marshall, and Walter G. Chapman[a)]
Department of Chemical and Biomolecular Engineering, Rice University, 6100 S. Main, Houston, Texas 77005, USA

(Received 20 May 2012; accepted 24 September 2012; published online 18 October 2012)

The understanding of phase behavior of copolymer brushes is of fundamental importance for the design of smart materials. In this paper, we have performed classical density functional theory calculations to study diblock copolymer brushes (A-B) in an explicit solvent which prefers the A block to B block. With increasing B-block length (N_B), we find a structural transition of the copolymer brush from mixed to collapsed, partial-exposed, and exposed structure, which is qualitatively consistent with experiments. The phase transitions are attributed to the interplay between entropic cost of folding copolymer brushes and enthalpic effect of contact between unlike components. In addition, we examine the effect of different parameters, such as grafting density (ρ_g), the bottom block length (N_A), and the chain length of solvent (N_S) on the solvent response of copolymer brushes. The transition chain length (N_B) increases with decreasing ρ_g and N_A, and a smaller solvent molecule makes the collapsed structure less stable due to its lower penetration cost. Our results provide the insight to phase behavior of copolymer brushes in selective solvents from a molecular view. © *2012 American Institute of Physics*. [http://dx.doi.org/10.1063/1.4757860]

I. INTRODUCTION

Grafting polymer brushes to surfaces[1–3] has proven to be a versatile method to tune surface properties with wide application in colloidal stabilization,[4] drug delivery,[5] or antifouling coatings.[6,7] Copolymer brushes,[8] due to phase separation between the blocks, are commonly utilized to create smart surfaces. In particular, the inclusion of a solvent can selectively expose one block of the copolymer brushes, resulting in changes of surface properties. Thus copolymer brushes attract much attention and have been studied extensively by experiments,[9–12] simulation,[13–15] and theoretical calculation.[16–19]

Recently, Xu *et al.*[12] studied the effect of block length on solvent response of poly(*n*-butyl methacrylate)-b-poly(2-(*N*,*N*′-dimethylamino)ethyl methacrylate) (PBMA-b-PDMAEMA) brushes. In their experiments, the diblock copolymer brushes with different top blocks (PDMAEMA) were immersed in hexane. Since hexane is a better solvent for PBMA than the PDMAEMA block, the copolymer brushes rearranged themselves into a different morphology, which was characterized by measuring the water contact angles. They found that as the top block (PDMAEMA) lengths increased, the response behavior of copolymer brushes transited from response region and partial-response region to non-response region. In the response region PBMA dominated the surface, while PDMAEMA occupied the surface in the non-response region. In the partial-response region, PBMA and PDMAEMA coexisted in the surface. However, the microstructure of copolymer brushes in different regions was not observed directly in the experiments and their explanation lacked theoretical support.

Computer simulation can be an alternative method to study the phase behavior of copolymer brushes from a molecular viewpoint, however, simulations become computationally demanding when explicit solvent is included in the system. Therefore, few simulations[13–15] of copolymer brushes are performed with an explicit solvent. To include the explicit solvent in the simulation, simulated annealing[13] or coarse-grained techniques[14,15] are commonly used to decrease computation time. For instance, Yin *et al.*[13] studied the phase behavior of copolymer brushes in selective solvents with the simulated annealing Monte Carlo method. They found complex morphology, such as the micelle, layer, and "flower," and also systematically studied the structure dependence on block length, grafting density, and solvent selectivity. Wang *et al.*[14] performed a single-chain-in-mean-field (SCMF) simulation of a coarse-grained model to investigate systematically the microphase separation of diblock copolymer brushes in selective solvents. They showed the phase diagram in terms of block fraction and grafting density. Also, Guskova *et al.*[15] used a coarse-grained dissipative particle dynamics simulation to study the morphological transitions of diblock copolymer brushes in selective solvents.

Self-consistent field theory (SCFT), which commonly imposes an incompressibility constraint, is also widely used in studying the complex phase behavior of copolymer brushes. For example, using SCFT, Ferreira *et al.*[16] studied the microstructure of diblock copolymer brushes in an implicit good solvent by varying the Flory-Huggins interaction parameter χ, a parameter to characterize the incompatibility between two blocks. A demixing transition is found for the diblock copolymer brushes (A-B) if χ is positive and solvent is poor. For a negative χ, the A and B blocks are attracted by each other. Thus the B segment can enter the A block region near the surface and the copolymer brushes become less stretched.

a)Author to whom correspondence should be addressed. Electronic mail: wgchap@rice.edu. Tel.: (1) 713.348.4900. Fax: (1) 713.348.5478.

Later, Meng *et al.*[17] used SCFT to quantify the explicit solvent response of diblock polymer brushes by the changes of surface-layer composition and brush height. The influence of different parameters, such as block fraction, block chain length, grafting density, incompatibility between two blocks, and solvent selectivity was also investigated.

Designing specific copolymer brushes for a targeted application is a delicate and challenging process because the response range of copolymer brushes is limited and depends on a large parameter space, such as grafting density, solvent properties, etc. Inspired by Xu *et al.*'s[12] experiments, we take advantage of density functional theory (DFT) to investigate the microstructure and response behavior of diblock copolymer brushes with the explicit solvent. Rooted in statistical mechanics, DFT is becoming a popular tool to model polymeric systems.[7,20–23] In comparison with simulation, DFT provides a more computationally efficient approach especially when the solvent is included explicitly. DFT has been extended to polymer brush systems by McCoy *et al.*[24,25] and later Jain *et al.*[26] Their results show that DFT is in good agreement with simulation and also follows the scaling relations proposed by Alexander[27] and de Gennes.[28] In our previous work,[29] we extended the work of Jain *et al.*[26] to study the surface switch of mixed polymer brushes with an implicit solvent. Now in this paper, DFT is further applied to model copolymer brushes with the explicit solvent. Different from other works, we focus on solvent response of diblock copolymer brushes (A-B) with different top block (B) length. Four different structures (mixed, collapsed, partial-exposed, and exposed) are found in this study. We also calculated the surface free energy for each structure to find the stable state. Another advantage of DFT over simulation is its ability to directly calculate surface free energy and thus to identify first order phase transitions in copolymer brushes. In addition, several important parameters, such as grafting density, bottom block length, and solvent size are systematically studied to present their effects on the phase transition of copolymer brushes. Consistent with Xu *et al.*'s[12] main experimental results, this study provides a theoretical basis for their conclusions. The paper is organized as follows: Sec. II explains the DFT model, Sec. III presents our results and the corresponding discussion, and Sec. IV summarizes our conclusions.

II. THEORY

We consider diblock AB copolymer brushes of chain length m_T in an explicit solvent (S) of chain length m_S. As an initial study, all the calculation in this work is performed in 1D, thus the possible lateral inhomogeneity in diblock copolymer brushes has been neglected. All the calculation in this work was carried out using TRAMONTO.[30] The copolymer brushes are modelled as freely jointed chains with one end tethered to a surface. According to Weeks-Chandler-Andersen perturbation theory, the interaction potential between segments can be described as a sum of a hard sphere reference, and a cut and shifted Lennard-Jones attraction,

$$u_{\alpha\beta}(r) = u^{ref}_{\alpha\beta}(r) + u^{att}_{\alpha\beta}(r), \tag{1}$$

where

$$u^{ref}_{\alpha\beta}(r) = \begin{cases} \infty & if \quad r < \sigma_{\alpha\beta} \\ 0 & if \quad r \geq \sigma_{\alpha\beta} \end{cases}, \tag{2}$$

and

$$u^{att}_{\alpha\beta}(r) = \begin{cases} u^{LJ}_{\alpha\beta}(r_{\min}) - u^{LJ}_{\alpha\beta}(r_c) & if \quad \sigma_{\alpha\beta} < r \leq r_{\min} \\ u^{LJ}_{\alpha\beta}(r) - u^{LJ}_{\alpha\beta}(r_c) & if \quad r_{\min} < r \leq r_c \end{cases}, \tag{3}$$

where

$$u^{LJ}_{\alpha\beta}(r) = 4\varepsilon_{\alpha\beta}\left[\left(\frac{\sigma_{\alpha\beta}}{r}\right)^{12} - \left(\frac{\sigma_{\alpha\beta}}{r}\right)^{6}\right]. \tag{4}$$

Here $r_{\min} = 2^{1/6}\sigma_{\alpha\beta}$ is the position of the Lennard-Jones potential minima and $r_c = 3.5\sigma_{\alpha\beta}$ is the cutoff distance. The interaction energy between segments are $\varepsilon_{AA} = \varepsilon_{BB} = \varepsilon_{SS} = \varepsilon_{AS} = 0.5$ for the like species, and $\varepsilon_{BS} = \varepsilon_{AB} = 0$ for the unlike species. The surface is a smooth hard wall that is neutral to the copolymer brush segments and solvent molecules.

In a previous work,[26] a specific DFT formalism for polymer brushes was developed. Briefly, the first segment of the tethered chain is half buried in the surface by setting the external field as

$$V^{ext}_1(z) = \begin{cases} v & if \quad z = 0 \\ \infty & otherwise \end{cases}, \tag{5}$$

where v is bonding energy.

For the other segments,

$$V^{ext}_i(z) = \begin{cases} \infty & if \quad z < \sigma_i/2 \\ 0 & otherwise \end{cases}. \tag{6}$$

In the grand canonical ensemble, the grand free energy (Ω) can be related to the intrinsic Helmholtz free energy functional (A) through the Legendre transform,

$$\Omega\left[\rho^{(T)}_i(r), \rho^{(S)}_i(r)\right] = A\left[\rho^{(T)}_i(r), \rho^{(S)}_i(r)\right] - \sum_{j=T,S}\sum_{i=1}^{m_l}\int dr' \rho^j_i(r')\left(\mu^j_i - V^{i,j}_{ext}(r')\right), \tag{7}$$

where $\rho^j_i(r)$ is the density, μ^j_i is the chemical potential, and $V^{i,j}_{ext}(r)$ is the external field. The first summation is over all chain j in the mixture (T, S) and the second summation is over all segments on chain j.

The main task in DFT is to construct the Helmholtz free energy functional. Based on thermodynamic perturbation theory (TPT), the total Helmholtz free energy functional can be decomposed into an ideal and excess contribution,

$$A\left[\rho^{(T)}_i(r), \rho^{(S)}_i(r)\right] = A^{id}\left[\rho^{(T)}_i(r), \rho^{(S)}_i(r)\right] + A^{ex,hs}\left[\rho^{(T)}_i(r), \rho^{(S)}_i(r)\right] + A^{ex,chain}\left[\rho^{(T)}_i(r), \rho^{(S)}_i(r)\right] + A^{ex,att}\left[\rho^{(T)}_i(r), \rho^{(S)}_i(r)\right]. \tag{8}$$

The ideal contribution comes from the ideal gas state of the atomic mixture (*id*). The excess contribution of the free

energy is due to excluded volume effects (*hs*), chain connectivity (*chain*), and long-range attractions (*att*).

The ideal gas functional is known exactly as

$$\beta A^{id}[\rho_\alpha] = \int dr_1 \sum_{q=T,S} \sum_{\alpha=1}^{m_q} \rho_\alpha^{seg}(r_1)\left(\ln \rho_\alpha^{seg}(r_1) - 1\right). \tag{9}$$

$A^{ex,hs}$ is calculated from the White-Bear version of fundamental measure theory[31–34] for a mixture of hard spheres,

$$\beta A^{ex,hs}[\rho_\alpha] = \int dr \Phi[n_\alpha(r)], \tag{10}$$

where $\Phi[n_\alpha(r)]$ is given by

$$\Phi[n_\alpha] = -n_0 \ln(1-n_3) + \frac{n_1 n_2}{1-n_3} - \frac{n_{v1}\cdot n_{v2}}{1-n_3} + \frac{n_2^3\left(1-n_{v2}^2/n_2^2\right)^3}{36\pi n_3^2(1-n_3)^2} \times (n_3 + (1-n_3)^2 \ln(1-n_3)), \tag{11}$$

and n_α are the weighted densities (or fundamental measures).

For the attraction term, some non-mean-field methods including the weighted density approximation[35–37] and quadratic density expansion[38,39] have been shown to be more accurate for simple fluids and have been successfully applied to several inhomogeneous systems such as square-well fluids,[40] Lennard-Jones fluids,[41] Yukawa potentials,[42,43] and Sutherland fluids.[44] However, these methods have not yet been extended to the polymer brush system.

For simplicity, the mean field approximation[45] is used for the attraction term,

$$\beta A^{ex,att}[\rho_\alpha] = \frac{1}{2} \sum_{q=T,S} \sum_{p=T,S} \sum_{\alpha=1}^{m_q} \sum_{\gamma=1}^{m_p} \int_{|r_2-r_1|>\sigma_{\alpha\gamma}} dr_1 dr_2 \beta u_{\alpha\gamma}^{att} \times (|r_2-r_1|)\rho_\alpha^{seg}(r_1)\rho_\gamma^{seg}(r_2). \tag{12}$$

The mean-field approximation has been validated with simulation for several polymer systems.[21,26,46,47]

Wertheim's first order thermodynamic perturbation theory (TPT1)[48–53] is used to calculate $A^{ex,chain}$ by forcing a mixture of spherical segments to bond in a specified order to form the copolymer or solvent molecules of interest. Thus, the chain contribution to the free energy functional is obtained by taking the complete bonding limit of an association free energy functional,

$$\beta A^{ex,assoc}[\rho_\alpha] = \int dr_1 \sum_{q=T,S} \sum_{\alpha=1}^{m_q} \rho_\alpha^{seg}(r_1) \times \sum_{A\in\Gamma^\alpha} \left(\ln X_A^\alpha(r_1) - \frac{X_A^\alpha(r_1)}{2} + \frac{1}{2}\right). \tag{13}$$

The first summation is over all the components (T, S), the second over all segments α in the corresponding chain, and the third over all the association sites on segment α as $\Gamma^{(\alpha)}$ is the set of all the associating sites on segment α. X_A^α denotes the fraction of segments of type α that are not bonded at their associating site A, which can be obtained by the law of mass action.[48,49]

The equilibrium density distribution of segments can be determined by minimizing the grand free energy, yielding a set of Euler-Lagrange (EL) equations

$$\frac{\delta\Omega}{\delta\rho_i^{(T)}} = \frac{\delta\Omega}{\delta\rho_i^{(S)}} = 0. \tag{14}$$

With the equilibrium density profile, the corresponding grand free energy can be obtained by simply substituting $\rho_i^j(r)$ into Eq. (7).

The EL equations are solved using Picard's iteration method with a damping factor.[26] The intial trial for the density distribution can be either a step density profile or an existing density profile. The iterations are repeated until the convergence criterion is satisfied (typically $|\rho_{new} - \rho_{old}| < 10^{-5}$). For the details of the numerical procedure of solving the above equations, please refer to our previous work.[21,26,29]

III. RESULTS

We have studied the solvent response properties of diblock copolymer A-B brushes (A is tethered to the surface). To minimize the large parameter space, we first fix the grafting density $\rho_g = 0.1$, length of A block $N_A = 50$, the chain length of solvent $N_S = 10$, and the solvent density $\rho_s = 0.8$. The surface is located at z = 0. The interaction energy is set such that the A block is attracted to the solvent, while the B block is solvent phobic. The length of B block (N_B) is varied to see its effect on the response properties. This parameter set is chosen to be qualitatively consistent with Xu *et al.*'s experiments.[12] Figure 1 gives an illustration of all the possible structures which can exist when the copolymer brushes are immersed in an explicit solvent: (a) mixed; (b) collapsed; (c) partial-exposed; and (d) exposed. Our results are consistent with Xu *et al.*'s[12] except the mixed structure (a). Xu *et al.*[12] divided the diblock copolymer brushes into three regions based on N_B: response region (similar to collapsed), partial-response region (partial-exposed), and non-response region (exposed).

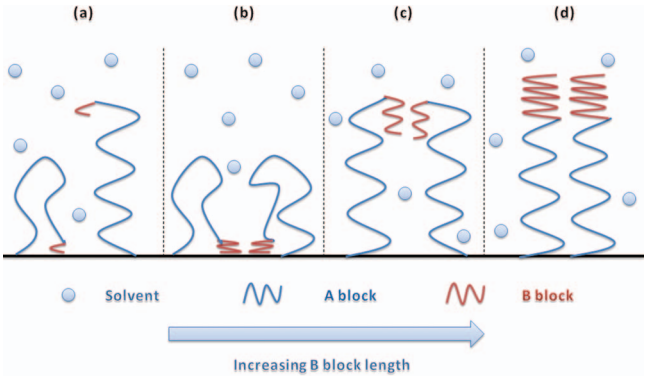

FIG. 1. Schematic illustration of solvent response of diblock copolymer brushes with different B block length. The length of A block is fixed. Red lines: A block. Blue lines: B block. A likes solvent, while B does not. The illustration shows all possible morphology of copolymer brushes immersed in explicit solvent: (a) mixed; (b) collapsed; (c) partial-exposed; and (d) exposed.

FIG. 2. Density profiles of solvated copolymer brushes with $\rho_g = 0.1$, $\rho_s = 0.8$, $N_A = 50$, and $N_S = 10$ at different lengths of B block: (a) $N_B = 2$; (b) $N_B = 6$; (c) $N_B = 8$; (d) $N_B = 20$; (a–d) show the corresponding microstructure previously illustrated in Figure 1. The density profile of B block is enlarged in the inset of (a) to present the mixed structure more clearly.

To provide detailed information about the different structures, the density profiles of the copolymer brushes (A-B) and solvent (S) with different lengths of B block are presented in Figure 2: (a) $N_B = 2$; (b) $N_B = 6$; (c) $N_B = 8$; (d) $N_B = 20$. Each case corresponds to structures given in Figure 1. We illustrate the morphology transition as the order of decreasing N_B. In Figure 2, the density profiles are plotted as a function of the distance from the tethered surface scaled by the diameter of the segment. When N_B is large, the B block cannot hide within the A block, and the exposed structure (d) is observed. Due to the complex interaction between copolymer brushes and solvents, there are two interfaces formed in (d): AS/B and B/A. The density profile of A block has strong oscillation near the surface and then forms a step like shape, which is commonly observed when homopolymer brushes are immersed in a good solvent. The solvent phobic B block arranges itself far from the surface in contact with the solvent. In addition, the solvent (S) penetrates into the polymer brush resulting in a fully extended solvent philic A block. Due to unfavorable S-B interactions on each side, the B block has been compressed significantly and forms the step like structure, where no solvent exists. When measuring contact angle, (d) will display the typical contact angle of B block due to the fact that B block consists of the surface outer layer and shields A block. This is the structure proposed by Xu *et al.*,[12] "the non-response region." When decreasing N_B to 8, the partial-exposed structure appears, as shown in (c). This type of structure is basically the same as the exposed structure except that the B block folds back toward the surface a little bit so that it is partly shielded by the A block. Although the DFT calculation is in 1D, this structure might imply that a surface-attached ripple, dimple micelle or perforated layer structure could be present, as has been observed in simulation. Determing the detailed equilibrium structure would require much more computationally intensive 3D DFT calculation. Therefore, the surface outer layer actually contains the mixture of A block and B block. Now if the contact angle is measured, an intermediate value between the contact angles of A block and B block is expected. The solvent can still penetrate into the polymer brushes surface region and even coexist with the solvent phobic B block. This is consistent with the so called "partial response region." When further decreasing N_B to 6, a structural transition from partial-exposed to collapsed morphology is observed. As shown in (b), B block collapses and forms a double layer near the surface due to unfavorable contact with solvent. The collapse of the B block further drags the A block to fold back toward the surface, which results in very high density in the polymer brush region. The solvent cannot easily penetrate into the polymer brush region, thus a depletion zone for the solvent appears. Now the

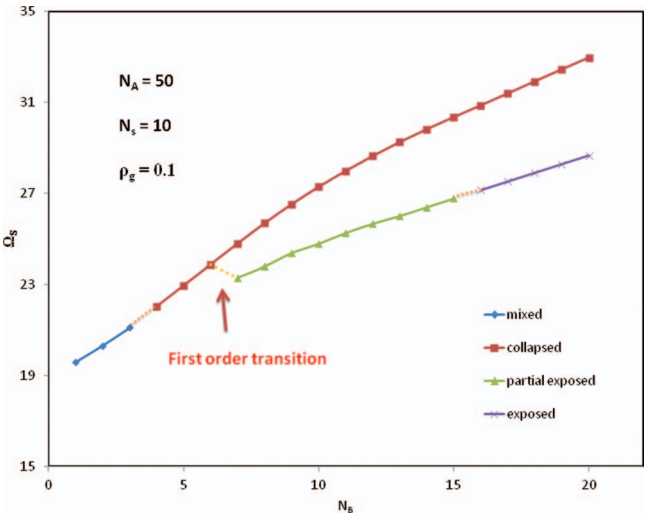

FIG. 3. Surface free energy (Ω_S) versus B block length (N_B) with $\rho_g = 0.1$, $\rho_s = 0.8$, $N_A = 50$, and $N_S = 10$. All the possible morphology (diamond: mixed, rectangle: collapsed, triangle: partial-exposed, cross: exposed) has been marked in the excess free energy diagram. The collapsed-partial-exposed structure phase transition happens at $N_B = 6$. The intersection between the collapsed-partial-exposed structure has a discontinuity of the slope, which indicates the first-order phase transition. (The dotted lines are used to connect different structures.)

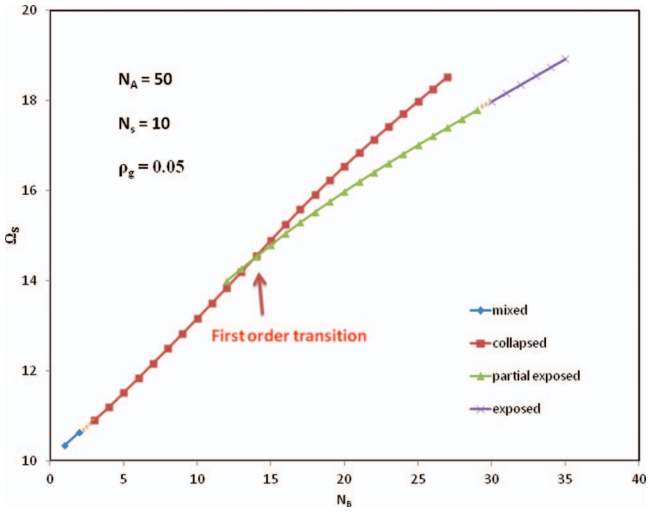

FIG. 4. Surface free energy (Ω_S) versus B block length (N_B) at lower grafting density $\rho_g = 0.05$. All the other parameters are the same with Fig. 3 except $\rho_g = 0.05$. $N_B = 12$ is considered as the transition chain length.

A block completely dominates the surface outer layer, and the contact angle is expected to be that of A block. This region is equal to "response region." When N_B is equal to 2, Figure 2(a) presents the mixed structure. The mixed structure is simply a combination between the collapsed and partial-exposed structure. Even though most of the B segments collapse toward the surface, a small fraction of B segments still stays far away from the surface and forms a partial-exposed structure. Such kind of a structure has not been observed in experiments, but our theory says that it is a possible stable structure when N_B and N_S are quite small.

We calculate the surface free energy (Ω_S) for each state, and plot it versus N_B to show the stable states of the system in Figure 3. The surface free energy is defined as $\Omega_S = \Omega - \Omega_{bulk}$, where Ω_{bulk} is the free energy of a bulk system of solvent with the same density. As shown in Figure 3, we can see the intersection (the dotted line pointed by the arrow), which has a discontinuity of the slope, indicating a possible first order phase transition from partial-exposed to collapsed structure. But it is hard to pinpoint the transition chain length N_B in Figure 3 because of the convergence of the calculations and the restriction to integer number of segments. The first order phase transition is more obvious in Figures 4 and 5. However, the transition from exposed to partial-exposed or from collapsed to mixed is not so obvious since they have a similar slope. When N_B is relatively large, the collapsed structure has a higher surface free energy than the exposed or partial-exposed structure. The state that has a lower surface free energy is proven to be more stable. Thus in the order of decreasing N_B, the copolymer brushes transit from exposed, partial-exposed, collapsed, and finally to a mixed structure. In this diblock copolymer brush system, the B block is solvent phobic and would rather stay near the grafting surface to hide from solvent, while the solvent philic A block likes to be immersed in the solvent. This is the enthalpic effect. On the other hand, the collapse of B block causes A block to fold back and forms a "U" shape. Thus a region with a high density of polymer brush and a low density of solvent appears, resulting in a large entropic penalty. The objective of the system is to minimize the surface free energy by striking a balance between the enthalpic effect and the entropic cost. When N_B is large, the entropic effect dominates and the exposed or partial-exposed structure is more stable. Meanwhile, a smaller N_B results in the enthalpic effect becoming the dominant factor, and the collapsed or mixed structures become more stable.

A larger parameter space can be employed to provide guidance for design of smart materials based on copolymer brushes. We mainly focus on the effect of grafting density ρ_g, A block length N_A, and chain length of solvent N_S in this paper. Grafting density is an important parameter for the polymer brushes and can be controlled in the experiments. In

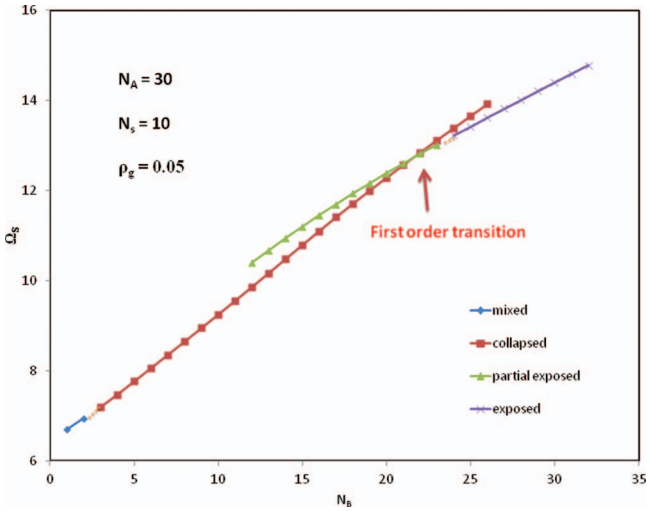

FIG. 5. Surface free energy (Ω_S) versus B block length (N_B) at shorter bottom block length $N_A = 30$. All the other parameters are the same with Fig. 4 except $N_A = 30$. $N_B = 22$ is considered as the transition chain length.

comparison to Figure 3, Figure 4 presents the relatively lower grafting density case $\rho_g = 0.05$. As we can see in Figure 4, all the structures presented for $\rho_g = 0.1$ can still be found, and the phase diagram is also similar. However, the transition chain length N_B increases from 6 to 12, as expected. The entropic cost resulting from folding of copolymer brushes increases with grafting density ρ_g, and it becomes a dominant factor in comparison to the enthalpic effect because of contact between unlike components. The result is actually consistent with our previous calculation of mixed polymer brushes with implicit solvent.[29] With inclusion of the explicit solvent, our conclusion that lower grafting density increases the transition chain length is further validated here.

Comparing Figures 4 and 5 shows the effect of bottom block length N_A on the solvent response behavior of copolymer brushes. All the parameters in Figure 5 are set the same as Figure 4 except that N_A decreases from 50 to 30. As we can see from Figure 5, the transition chain length N_B increases from 12 to 22 as N_A is decreased. It seems that the copolymer brush with a shorter bottom block length N_A can form a "U" shape (collapsed structure) easier. For example, if the top block length N_B is 20, then partial-exposed structure is the stable one in Figure 4 while Figure 5 presents the collapsed structure. However, experiments[12] show a scaling relationship that the ratio between the lengths of two blocks (N_A/N_B) determines the contact angle. One reason for the difference is that our model system is not exactly the same as the one in the experiments. In the experiments, the removal of solvent is necessary before measuring the contact angle. However, in our calculation, the copolymer brushes are always immersed in the explicit solvent. Thus it is possible that structural change occurs in the drying process. The other reason may be related to polymer brush flexibility; in the DFT model (based on a first order thermodynamic perturbation theory), chains are freely jointed, which is not true for real systems. Recently, Marshall and Chapman[54] extended the DFT model to include the bond rigidity by implementing second order thermodynamic perturbation theory (TPT2). By modeling the polymer chain as semiflexible, it may be possible to improve agreement between the theoretical calculation and the contact angle measuring experiments for the bottom block length effect.

The chain length of solvent N_S is also an interesting parameter to employ, which most of the experiments and simulations have neglected. For example, if in the experiments one switches the top and bottom block of the copolymer brushes, and water instead of hexane is used to treat the copolymer brushes, then a different result might be obtained. Such kind of a prediction can easily be made by the DFT theory. Now the chain length of solvent N_s is decreased from 10 (Figure 2) to 1 (Figure 6) to show its effect on the phase behavior of copolymer brushes. All the other parameters in Figure 6 are the same with Figure 2. Interestingly, the collapsed structure is not a stable state at any value of N_B, even though it can still exist as an unstable structure. There is a direct transition from the partial-exposed to mixed structure, instead of an intermediate collapsed structure. No first order phase transition is found since the slopes of mixed and partial-exposed structures are almost the same. However, as shown in Figure 6,

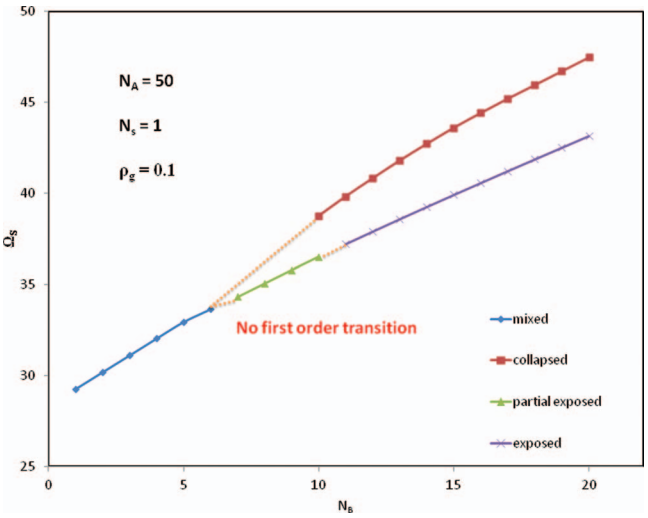

FIG. 6. Surface free energy (Ω_S) versus B block length (N_B) at smaller solvent $N_S = 1$. All the other parameters are the same with Fig. 3 except $N_S = 1$.

the slope of collapsed structure is still different with the other structures'. Usually it is easier for the smaller size solvent to penetrate into the polymer brush region due to the lower entropic cost. The strong penetration of solvent makes some fraction of A block become fully extended and thus B block has to stay far away from the grafting surface. This explains why the mixed structure is the preferred one in comparison with the fully collapsed structure for the smaller N_s case.

It is of interest to compare our results with previous simulation[13–15] and SCFT[17] calculations. Quantitative comparison is difficult because of the different molecular models used. Qualitatively, as shown in simulation, the copolymer brushes transited from the layer, perforated layer, and ripple micelle to dimple micelle with decrease of B block length. Compared with our work, the layer structure is the same as the exposed structure, while the other three correspond to the partial-exposed structure. The collapsed and mixed structures are not found in simulation. The missing collapsed structure is not surprising since all the simulation is performed with only a single bead solvent. According to our previous conclusion, the collapsed structure became unstable as the solvent size decreased from 10 (Figure 2) to 1 (Figure 6). In addition, 1D calculation of SCFT[17] only showed the partial-exposed structure.

To provide more guidance for the experimental design of the copolymer brushes, a larger parameter space such as solvent quality or temperature, solvent density, solvent selectivity, and the chain flexibility should be explored. In this paper, we have investigated several important parameters to show how the diblock copolymer brushes respond and self-organize after the solvent treatment.

IV. CONCLUSIONS

Both copolymer brushes and mixed polymer brushes are considered as natural materials to fabricate smart surfaces. Our previous work[29] has demonstrated that DFT can capture the competition between entropic cost and enthalpic effect in

the surface switch of mixed polymer brushes. However, the packing effect of solvent molecules was neglected due to an implicit solvent assumption in the model. In this study, the phase behavior of diblock copolymer brushes in explicit solvent is examined by DFT. Compared with molecular simulation, DFT has the great advantage of computational efficiency, which makes it easy to include explicit solvent. Consistent with experimental observation, we have found four different structures: mixed, collapsed, partial-exposed, and exposed. The transition chain length increases with decreasing grafting density, which is similar to the mixed polymer brushes case.[29] Moreover, the collapsed structure becomes less stable on decreasing the chain length of solvent. The approach is demonstrated as an alternative to simulation or SCFT methods that is capable of representing the complex phase behavior of copolymer brushes by accurately modeling the interplay between the entropic and enthalpic effects.

Our work is based on the assumption of one dimension of inhomogeneity thus excluding a possible higher dimension structure, which may be observed in simulation or experiments. But it is evident that DFT can provide the physical insight and useful guidance for the design of smart surfaces modified with copolymer brushes for targeted application.

ACKNOWLEDGMENTS

Financial support for this work was provided by the Robert A. Welch Foundation (Grant No. C-1241) and by the National Science Foundation (CBET-0756166).

We thank Sandia National Laboratories for use of TRAMONTO software.

We thank the reviewers for the constructive suggestions.

[1] S. T. Milner, Science **251**(4996), 905 (1991).
[2] B. Zhao and W. J. Brittain, Prog. Polym. Sci. **25**(5), 677 (2000).
[3] P. Mansky, Y. Liu, E. Huang, T. P. Russell, and C. J. Hawker, Science **275**(5305), 1458 (1997).
[4] P. Pincus, Macromolecules **24**(10), 2912 (1991).
[5] I. Y. Galaev and B. Mattiasson, Trends Biotechnol. **17**(8), 335 (1999).
[6] K. Glinel, A. M. Jonas, T. Jouenne, J. Leprince, L. Galas, and W. T. S. Huck, Bioconjugate Chem. **20**(1), 71 (2009).
[7] X. Xu, D. Cao, and J. Wu, Soft Matter **6**(19), 4631 (2010).
[8] M. A. C. Stuart, W. T. S. Huck, J. Genzer, M. Mueller, C. Ober, M. Stamm, G. B. Sukhorukov, I. Szleifer, V. V. Tsukruk, M. Urban, F. Winnik, S. Zauscher, I. Luzinov, and S. Minko, Nature Mater. **9**(2), 101 (2010).
[9] B. Zhao, W. J. Brittain, W. S. Zhou, and S. Z. D. Cheng, J. Am. Chem. Soc. **122**(10), 2407 (2000).
[10] B. Zhao and W. J. Brittain, J. Am. Chem. Soc. **121**(14), 3557 (1999).
[11] J. B. Kim, W. X. Huang, M. L. Bruening, and G. L. Baker, Macromolecules **35**(14), 5410 (2002).
[12] C. Xu, T. Wu, C. M. Drain, J. D. Batteas, M. J. Fasolka, and K. L. Beers, Macromolecules **39**(9), 3359 (2006).
[13] Y. Yin, P. Sun, B. Li, T. Chen, Q. Jin, D. Ding, and A.-C. Shi, Macromolecules **40**(14), 5161 (2007).
[14] J. Wang and M. Mueller, Macromolecules **42**(6), 2251 (2009).
[15] O. A. Guskova and C. Seidel, Macromolecules **44**(3), 671 (2011).
[16] P. G. Ferreira and L. Leibler, J. Chem. Phys. **105**(20), 9362 (1996).
[17] D. Meng and Q. Wang, J. Chem. Phys. **130**(13), 134904 (2009).
[18] E. B. Zhulina, C. Singh, and A. C. Balazs, Macromolecules **29**(19), 6338 (1996).
[19] E. B. Zhulina, C. Singh, and A. C. Balazs, Macromolecules **29**(25), 8254 (1996).
[20] J. Z. Wu, AIChE J. **52**(3), 1169 (2006).
[21] S. Jain, A. Dominik, and W. G. Chapman, J. Chem. Phys. **127**(24), 244904 (2007).
[22] C. P. Emborsky, Z. Feng, K. R. Cox, and W. G. Chapman, Fluid Phase Equilib. **306**(1), 15 (2011).
[23] S. Tripathi and W. G. Chapman, Phys. Rev. Lett. **94**(8), 087801 (2005).
[24] J. D. McCoy, Y. Ye, and J. G. Curro, J. Chem. Phys. **117**(6), 2975 (2002).
[25] Y. Ye, J. D. McCoy, and J. G. Curro, J. Chem. Phys. **119**(1), 555 (2003).
[26] S. Jain, P. Jog, J. Weinhold, R. Srivastava, and W. G. Chapman, J. Chem. Phys. **128**(15), 154910 (2008).
[27] S. Alexander, J. Phys. (France) **38**(8), 983 (1977).
[28] P. G. Degennes, *Scaling Concepts in Polymer Physics* (Cornell University, Ithaca, NY, 1979).
[29] K. Gong and W. G. Chapman, J. Chem. Phys. **135**(21), 214901 (2011).
[30] See https://software.sandia.gov/tramonto/index.html for TRAMONTO.
[31] Y. Rosenfeld, Phys. Rev. Lett. **63**(9), 980 (1989).
[32] A. Oleksy and J.-P. Hansen, Mol. Phys. **104**(18), 2871 (2006).
[33] R. Roth, R. Evans, A. Lang, and G. Kahl, J. Phys.: Condens. Matter **14**(46), 12063 (2002).
[34] Y. X. Yu and J. Z. Wu, J. Chem. Phys. **117**(22), 10156 (2002).
[35] T. H. Yoon and S. C. Kim, Phys. Rev. E **58**(4), 4541 (1998).
[36] C. N. Patra and S. K. Ghosh, J. Chem. Phys. **116**(19), 8509 (2002).
[37] S. Q. Zhou, J. Phys. Chem. B **106**(31), 7674 (2002).
[38] Y. P. Tang, J. Chem. Phys. **121**(21), 10605 (2004).
[39] Y. P. Tang and J. Z. Wu, Phys. Rev. E **70**(1), 011201 (2004).
[40] Z. Jin, Y. Tang, and J. Wu, J. Chem. Phys. **134**(17), 174702 (2011).
[41] J. G. Mi, Y. P. Tang, C. L. Zhong, and Y. G. Li, J. Chem. Phys. **124**(14), 144709 (2006).
[42] Y.-X. Yu and L. Jin, J. Chem. Phys. **128**(1), 014901 (2008).
[43] Y. P. Tang, Y. Z. Lin, and Y. G. Li, J. Chem. Phys. **122**(18), 184505 (2005).
[44] J. Mi, Y. Tang, and C. Zhong, J. Chem. Phys. **128**(5), 054503 (2008).
[45] J. P. Hansen and I. R. McDonald, *Theory of Simple Liquids* (Academic, San Diego, CA, 1986).
[46] D. P. Cao and J. Z. Wu, Macromolecules **38**(3), 971 (2005).
[47] Z. D. Li, D. P. Cao, and J. Z. Wu, J. Chem. Phys. **122**(17), 174708 (2005).
[48] W. G. Chapman, Ph.D. dissertation, Cornell University, 1988.
[49] C. J. Segura, W. G. Chapman, and K. P. Shukla, Mol. Phys. **90**(5), 759 (1997).
[50] M. S. Wertheim, J. Stat. Phys. **35**(1-2), 19 (1984).
[51] M. S. Wertheim, J. Stat. Phys. **35**(1-2), 35 (1984).
[52] M. S. Wertheim, J. Stat. Phys. **42**(3-4), 459 (1986).
[53] M. S. Wertheim, J. Stat. Phys. **42**(3-4), 477 (1986).
[54] B. D. Marshall and W. G. Chapman, J. Phys. Chem. B **115**(50), 15036 (2011).